Acta Crystallographica Section F
Structural Biology and Crystallization Communications
ISSN 1744-3091

The 1.75 Å resolution structure of fission protein Fis1 from *Saccharomyces cerevisiae* reveals elusive interactions of the autoinhibitory domain

James E. Tooley,[a] Victor Khangulov,[b] Jonathan P. B. Lees,[a] Jamie L. Schlessman,[c] Maria C. Bewley,[d] Annie Heroux,[e] Jürgen Bosch[f]* and R. Blake Hill[a,g]*

[a]Department of Biology, Johns Hopkins University, Baltimore, MD 21218, USA, [b]Department of Biophysics, Johns Hopkins University, Baltimore, MD 21218, USA, [c]Chemistry Department, US Naval Academy, Annapolis, MD 21402, USA, [d]Department of Biochemistry and Molecular Biology, Pennsylvania State University College of Medicine, Hershey, PA 17033, USA, [e]National Synchrotron Light Source, Brookhaven National Laboratory, Upton, NY 11973, USA, [f]Department of Biochemistry and Molecular Biology, Johns Hopkins Bloomberg School of Public Health, Baltimore, MD 21205, USA, and [g]Department of Chemistry, Johns Hopkins University, Baltimore, MD 21218, USA

Correspondence e-mail: jubosch@jhsph.edu, hill@jhu.edu

Received 30 May 2011
Accepted 20 July 2011

PDB Reference: Fis1 cytoplasmic domain, 3o48.

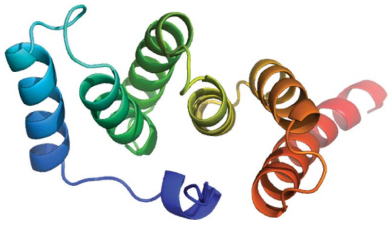

Fis1 mediates mitochondrial and peroxisomal fission. It is tail-anchored to these organelles by a transmembrane domain, exposing a soluble cytoplasmic domain. Previous studies suggested that Fis1 is autoinhibited by its N-terminal region. Here, a 1.75 Å resolution crystal structure of the Fis1 cytoplasmic domain from *Saccharomyces cerevisiae* is reported which adopts a tetratricopeptide-repeat fold. It is observed that this fold creates a concave surface important for fission, but is sterically occluded by its N-terminal region. Thus, this structure provides a physical basis for autoinhibition and allows a detailed examination of the interactions that stabilize the inhibited state of this molecule.

1. Introduction

Mitochondria and peroxisomes undergo membrane fission that is crucial for organelle propagation, cellular homeostasis and human health (Chan, 2007). The protein Fis1 is implicated in the fission of both organelles, which possibly occurs by the direct recruitment of a dynamin-related mechanoenzyme, Dnm1, the activity of which is modulated by adaptor proteins such as Mdv1 and Caf4 in budding yeast (Motley *et al.*, 2008; Wells *et al.*, 2007; Zhang & Chan, 2007; Schrader, 2006; Griffin *et al.*, 2005; Koch *et al.*, 2005; Dohm *et al.*, 2004; Cerveny & Jensen, 2003; Suzuki *et al.*, 2003; Yoon *et al.*, 2003; Tieu *et al.*, 2002). Fis1 is composed of two domains: a C-terminal transmembrane domain that anchors the protein to the organelle and a ∼16 kDa cytosolic domain thought to recruit fission factors to sites of membrane scission.

NMR and X-ray structures of mammalian and yeast Fis1, both lacking the C-terminal transmembrane domain (Fis1ΔTM), have been solved and show that the cytosolic domain adopts a tetratricopeptide-like (TPR-like) fold (Zhang & Chan, 2007; Dohm *et al.*, 2004; Suzuki *et al.*, 2003, 2005). The TPR fold is a common protein–protein interaction fold (Blatch & Lässle, 1999; Cortajarena & Regan, 2006) that creates a concave surface lined with evolutionarily conserved residues that have been shown to be functionally important (Dohm *et al.*, 2004; Suzuki *et al.*, 2003, 2005). The structure of this fold is consistent with the proposed role of Fis1 in protein recruitment (Tieu & Nunnari, 2000; Mozdy *et al.*, 2000; Fekkes *et al.*, 2000). The solution structures of Fis1ΔTM from human (Suzuki *et al.*, 2003), mouse (PDB entry 1iyg; W. Ohashi, H. Hirota, T. Yamazaki, S. Koshiba, T. Hamada, M. Yoshida & S. Yokoyama, unpublished work) and budding yeast show the protein to be monomeric (Suzuki *et al.*, 2005), whereas the crystal structure of human Fis1 was found to be dimeric (Dohm *et al.*, 2004). The exact role of the Fis1 monomer and higher-order species is unknown, although cross-linking and blue native PAGE studies have found the self-association of Fis1 to be mediated in part by the cytosolic domain (Serasinghe & Yoon, 2008; Jofuku *et al.*, 2005).

A notable difference that is observed between Fis1 structures is the orientation of the N-terminal region, an autoinhibitory domain, also called the Fis1 arm (Wells *et al.*, 2007; Suzuki *et al.*, 2005; Serasinghe &

Yoon, 2008; Karren *et al.*, 2005). The Fis1 arm appears to be either structured in a manner that sterically occludes access to the concave surface or disordered in a manner that would allow access. The autoinhibitory nature of the Fis1 arm has been observed in both mammalian and yeast studies, where it mediates self-association (Serasinghe & Yoon, 2008). In yeast, it has also been shown to recruit both Dnm1 and Mdv1 (Wells *et al.*, 2007; Suzuki *et al.*, 2005; Karren *et al.*, 2005). In a cocrystal structure of yeast Fis1ΔTM containing peptides derived from either of the fission adaptor proteins Mdv1 or Caf4, the Fis1 arm appeared to contribute directly to ligand binding (Zhang & Chan, 2007). In biochemical experiments with yeast Fis1, the Fis1 arm inhibits Dnm1 binding (Wells *et al.*, 2007). Hydrogen–deuterium exchange and chemical modification experiments suggest that the Fis1 arm is dynamic on a timescale of seconds to minutes, modulating access to the functionally critical region. These observations are consistent with the dynamic view of the Fis1 arm in regulating protein–protein interactions (Picton *et al.*, 2009). Thus, the Fis1 arm appears to be an important regulator for binding the mechanoenzyme Dnm1.

The structural differences in the autoinhibitory domain of Fis1 and its existence in different oligomeric states have motivated us to pursue crystallization trials under conditions that might sample these different states. Here, we report the X-ray crystallographic structure of the cytosolic domain of the budding yeast Fis1 (Fis1ΔTM) at a resolution of 1.75 Å. Unlike the structure of the human ortholog, which was dimeric, the yeast protein adopted a monomeric conformation in the crystal. We find good electron density for residues 5–16 of the autoinhibitory Fis1 arm, which occludes a putative binding surface. Analysis of this structure in light of the structures of complexes with peptides from Mdv1 and Caf4 reveals that modest conformational changes are induced in Fis1 upon ligand binding. The high resolution of this structure allows a better evaluation of the interactions that stabilize the Fis1 arm into the concave surface than previously possible. This will help guide future mutagenesis efforts in functional studies. The atomic coordinates and structure factors have been deposited in the Protein Data Bank (PDB; http://www.pdb.org; accession code 3o48).

Table 1
Crystallographic data for Fis1(1–127).

Values in parentheses are for the highest resolution shell.

Data collection	
Space group	$P4_32_12$ [No. 89]
Unit-cell parameters (Å)	a = 46.020, c = 139.220
Wavelength (Å)	1.0
Resolution range (Å)	20–1.75 (1.80–1.75)
Total No. of reflections	708425
No. of observed reflections	24986
Completeness (%)	95.8 (94.5)
Multiplicity	23.26 (26.16)
$\langle I/\sigma(I)\rangle$	10.21 (6.84)
$R_{\rm merge}$ on I (%)	32.4 (50.5)
σ cutoff	0.0
Model and refinement statistics	
Resolution range (Å)	20–1.75
Total No. of reflections	14487
No. of reflections in test set	807
Completeness (%)	100
Stereochemical parameters	
Restraints (r.m.s. observed)	
Bond lengths (Å)	0.007
Bond angles (°)	0.85
Average isotropic B value (Å^2)	22.9
ESU based on R value	0.113
No. of residues	140
No. of atoms	1339
No. of water molecules	231
Average B value for water molecules (Å^2)	27.7
$R_{\rm all}$ (%)	0.166
$R_{\rm work}$ (%)	0.165
$R_{\rm free}$ (%)	0.187
Wilson B (Å^2)	22.7
Mosaicity (°)	0.232
MolProbity Ramachandran analysis	
Favored region (%)	98.5
Allowed region (%)	100
PDB code	3o48

2. Materials and methods

2.1. Protein expression and purification

A pET-29b vector (EMD Biosciences) containing the gene encoding Fis1(1–127) from *Saccharomyces cerevisiae* with a C-terminal hexahistidine tag that was cleavable by tobacco etch virus (TEV) protease was kindly provided by Drs Emily Coonrod and Janet M. Shaw. The plasmid was transformed into Rosetta(DE3) cells (EMD Biosciences) for overexpression. Cells were grown in lysogeny broth at 310 K to an OD_{600} of ∼0.7, when protein expression was induced by addition of 0.5 m*M* IPTG. Cells were grown for 16–24 h at 293 K with vigorous shaking and were collected by centrifugation at 6100*g* for 10 min. The resulting cell pellet was resuspended in buffer *A* (20 m*M* sodium phosphate, 250 m*M* NaCl and 20 m*M* imidazole pH 7.4) at 0.2 g ml^{-1} and frozen until lysis. For lysis, cells were thawed and one tablet of protease-inhibitor cocktail (Roche Applied Science) per 80 ml was added. Cells were homogenized using an EmulsiFlex-C3 cell homogenizer (Avestin), and bovine pancreas DNase I (Roche Applied Science) and $MgCl_2$ were added to final concentrations of 1 mg ml^{-1} and 1 m*M*, respectively. The homogenate was centrifuged at 31 000*g* for 45 min and the resulting supernatant was applied onto a HisTrap HP column (GE Healthcare) charged with Ni^{2+} and equilibrated in buffer *A*. Protein was eluted with a gradient of 20–500 m*M* imidazole and fractions containing Fis1 were pooled and treated with His-tagged TEV protease (1:50 molar ratio) overnight at 277 K. The fractions were then reapplied to the HisTrap HP column, followed by size-exclusion chromatography using a HiLoad 16/60 Superdex 75 prep-grade column (GE Healthcare) that was equilibrated with 50 m*M* sodium phosphate, 184 m*M* NaCl, 5 m*M* ethylenediaminetetraacetic acid (EDTA) and 2 m*M* dithiothreitol (DTT) pH 7.4. Purified protein was concentrated to 13.5 mg ml^{-1} in 50 m*M* Tris, 50 m*M* NaCl pH 7.5.

2.2. Crystallization, data collection and structure determination

Crystallization conditions for Fis1ΔTM were initially screened using Crystal Screen, Crystal Screen 2, Crystal Screen Cryo and PEG/Ion (Hampton Research) *via* sitting-drop vapor diffusion at 298 K with drops consisting of 1 µl protein solution and 1 µl reservoir buffer. The reservoir volume was 250 µl. Only crystals derived from the cleaved protein resulted in high-quality diffraction data; the uncleaved protein (and other constructs with shorter and longer N- and C-termini) crystallized but resulted in anisotropic diffraction. Tetragonal crystals were obtained using 11.8%(*w*/*v*) PEG 8K, 0.2 *M* ammonium sulfate and were frozen directly in liquid nitrogen. Diffraction data were recorded from a native crystal at 100 K through the 'Mail-In Data Collection' program offered at the National Synchrotron Light Source (Robinson *et al.*, 2006) on beamline X25. The data were processed and scaled using *XDS*/*XSCALE* (Kabsch, 2010). A molecular-replacement solution was found and initially refined with *BALBES* (Long *et al.*, 2008) using the structure of yeast Fis1 in complex with a fragment of Mdv1 (PDB entry 2pqn, chain *A*; Zhang & Chan, 2007) as the search model. Initial and subsequent model building were performed in *Coot* (Emsley *et al.*, 2010)

and atomic models were refined to convergence using *REFMAC* including TLS (translation/libration/screw) refinement (Winn *et al.*, 2003; Murshudov *et al.*, 2011) using resolution limits of 20–1.75 Å. TLS groups derived from the *TLSMD* web server (Painter & Merritt, 2005) were used throughout the refinement procedure, employing the restrained maximum-likelihood protocol with H atoms added in riding positions. The first four residues were omitted from the final model as no supportive electron density was observed to allow model building. Waters were added to an $F_o - F_c$ difference density map using default values in *Coot* (Emsley *et al.*, 2010) for the water-picking routine (σ = 1.0). The coordinates were refined to a final R_{work} of 16.5% (R_{free} = 18.8%) with excellent stereochemistry (Table 1). Validation of the model was carried out using *MolProbity* (Chen *et al.*, 2010). Structural comparisons were made and figures were generated using *PyMOL* (DeLano, 2002).

2.3. Structural analysis

R.m.s.d. analyses between PDB entries 3o48, 1y8m (Suzuki *et al.*, 2005), 2pqn (Zhang & Chan, 2007) and 2pqr (Zhang & Chan, 2007) were made using scripts in *PyMOL* (DeLano, 2002). Identification of hydrogen bonds and hydrophobic interactions was performed manually and was confirmed with the *DIMPLOT* feature within the *LIGPLOT* v.4.5.3 software (Wallace *et al.*, 1995). Default *LIGPLOT* parameters were used to determine the interactions between residues 5–16 and 17–127 of one monomer (distance and angular criteria for hydrogen bonds and a 3.9 Å distance cutoff for hydrophobic interactions as specified in Wallace *et al.*, 1995).

3. Results and discussion

3.1. Structure of yeast Fis1(1–127)

The crystal structure of Fis1ΔTM (1–127) was solved at 1.75 Å resolution (Fig. 1, Table 1). The tetragonal crystal form (space group $P4_32_12$) contains one molecule in the asymmetric unit and is composed of an antiparallel array of six α-helices that create two TPR motifs formed between α2–α3 and α4–α5, similar to the NMR structural ensemble (Fig. 1). TPR motifs in proteins typically range from 3–16 repeats with an additional 'capping helix' found C-terminal to the final repeat (D'Andrea & Regan, 2003). The architecture of Fis1 is different in that it is composed of only two repeats which are both flanked by 'capping helices' (α1 and α6). The minimum number of repeats required to create a concave binding surface has been postulated to be three (D'Andrea & Regan, 2003). However, we find in Fis1 that two TPR motifs with capping helices are sufficient to create a concave surface which cradles the Fis1 arm intramolecularly. We interpret this data to support the idea that two TPR motifs are

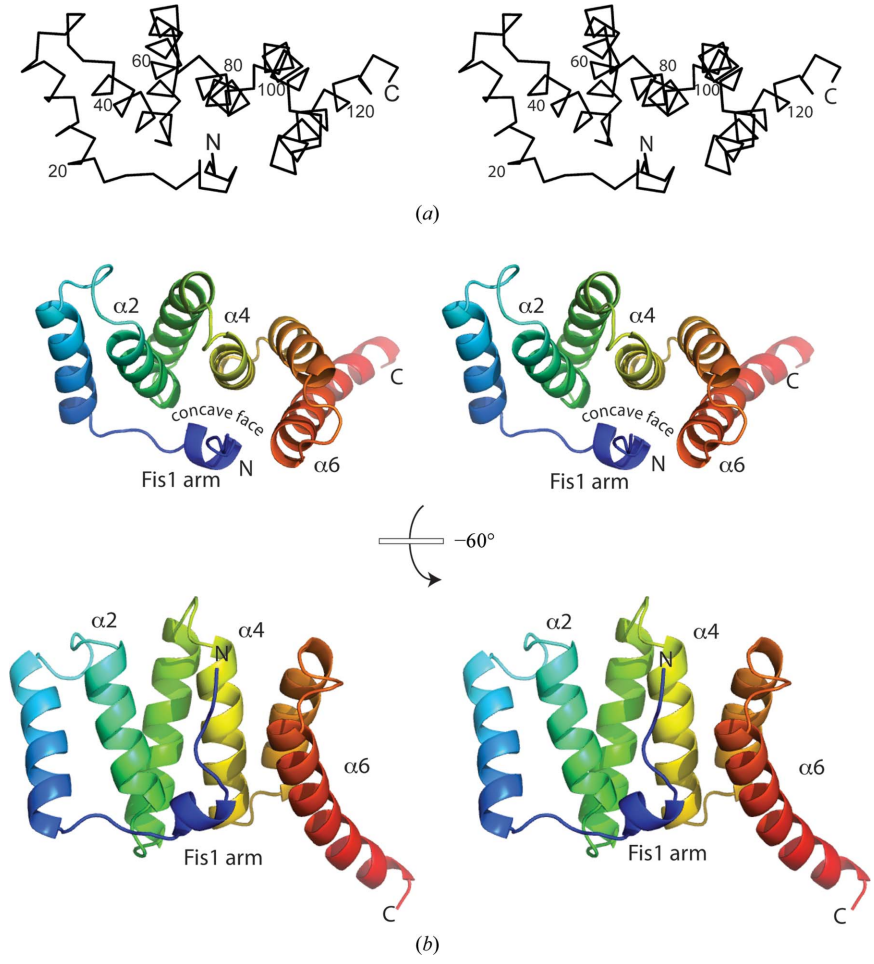

Figure 1
Yeast Fis1ΔTM adopts a TPR-like fold. (*a*) Stereoview of the C^{α} trace of Fis1 with every 20th residue labeled. Note that no electron density was observed for residues 1–5, which are not depicted. (*b*) A stereoview cartoon of the Fis1 backbone with the autoinhibitory domain, or Fis1 arm, in blue and the remainder of the molecule rainbow colored from blue to red from the N-terminus to the C-terminus. The first tetratricopeptide repeat consists of helices 2–3 and the second repeat consists of helices 4–5. The bottom panel was obtained by a −60° rotation along the *x* axis of the structure in the top panel. This figure was generated in *PyMOL* (DeLano, 2002).

sufficient for ligand binding. This has recently been shown to be true for human Fis1ΔTM, which also contains only two TPR motifs (Serasinghe *et al.*, 2010).

3.2. The autoinhibitory Fis1 arm

The removal of the first 16 residues (the Fis1 arm) of Fis1 allows a robust biochemical interaction with Dnm1 (Wells *et al.*, 2007) and results in altered morphology from impaired recruitment of Mdv1 and presumably Dnm1 (Suzuki *et al.*, 2005; Karren *et al.*, 2005). A structural model that might explain these data would involve the Fis1 arm dynamically mediating access to its concave surface, which is supported by the conformational heterogeneity of the NMR ensemble (r.m.s.d. of 3.18 Å for the C^{α} atoms of residues 1–16 *versus* 0.69 Å for the C^{α} atoms of residues 20–125; Suzuki *et al.*, 2005), hydrogen–deuterium exchange and chemical modification experiments (Picton *et al.*, 2009). In our crystal structure, residues 5–16 of the Fis1 arm are well defined, with an average C^{α}-atom *B* factor of 29.5 $Å^2$ (that for residues 5–127 is 19.2 $Å^2$ for C^{α} atoms; Fig. 2). Residues 1–4 of the arm appeared to be disordered in the structure and may be disposable for function, since expression of Fis1 lacking these residues (ΔN5-Fis1) in a *fis1* null strain rescues mitochondrial morphology, whereas an armless construct (ΔN15-Fis1) does not (Suzuki *et al.*, 2005).

The high quality of the data allows the inspection of structural features that may be important in stabilizing the interaction between the Fis1 arm and the concave surface (Figs. 2 and 3*a*). We find that Lys89 from the second TPR motif is hydrogen bonded to the backbone carbonyl of Ala13 in the Fis1 arm and the backbone carbonyls of Ile50 and Lys51 in the first TPR motif (Fig. 2*b*). This interaction is notable because we find a similar interaction in the human Fis1 structure (Dohm *et al.*, 2004). Other interactions also serve to stabilize the arm in the autoinhibitory state, including (i) the carboxamide side chain of Gln112 on α6, which engages in a bifurcated hydrogen-bonding interaction with the backbone peptide bond of Trp7 in the Fis1 arm (Fig. 2*c*); (ii) the backbone carbonyl of Pro8, which appears to be hydrogen bonded to the tyrosine hydroxyl of Tyr81; and (iii) a turn of α-helix formed between residues 10 and 16 that is stabilized by a salt bridge between the side chains of Lys11 and Glu15 (Fig. 2*a*). These and other interactions were not revealed by *LIGPLOT* (Wallace *et al.*, 1995) analysis of the lowest-energy NMR-derived structure (Fig. 3*b*), which may be a consequence of the dynamic nature of the Fis1 arm (Picton *et al.*, 2009). In the NMR structure a hydrogen bond was found between Asp12 and Lys51, whereas this interaction was not found in our structure (Figs. 3*b* and 3*c*). We predict that mutations to the residues highlighted here will destabilize the arm and its interaction with the concave surface and decrease the degree to which the arm prevents Dnm1 binding.

3.3. Comparison of the crystal complex of Fis1 and Caf4/Mdv1

Fis1 recruits the fission-adaptor proteins Caf4 and Mdv1 to sites of scission, where they act in regulating the fission mechanoenzyme

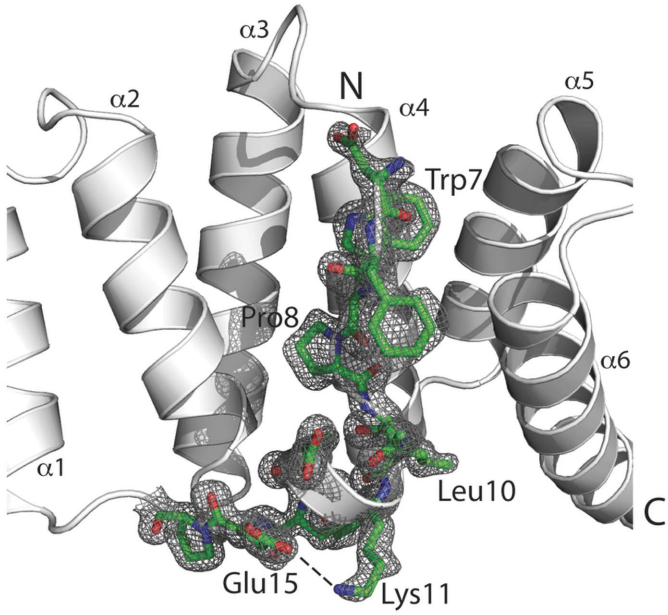

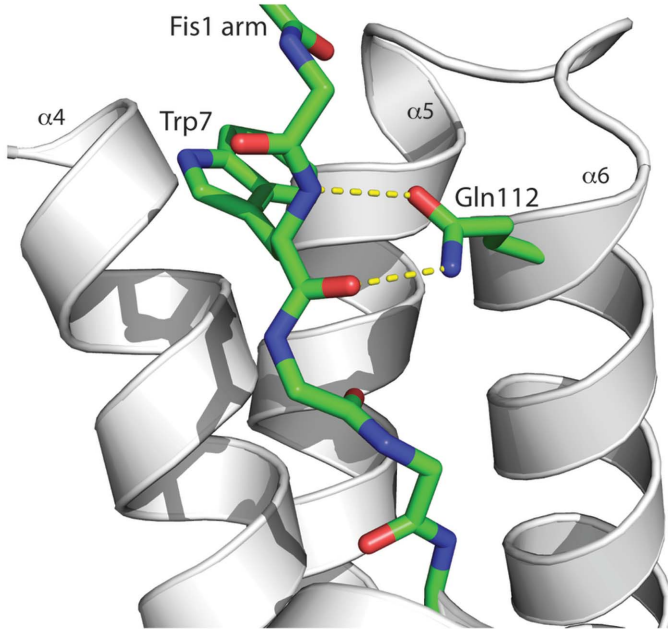

Figure 2
Multiple interactions contribute to stabilizing the Fis1 arm–concave surface interaction. (*a*) The final σ_A-weighted $2F_o - F_c$ electron-density map displaying residues 5–16 in the autoinhibitory Fis1 arm calculated at 1.75 Å resolution and contoured at 1σ. (*b*) Expanded view of the hydrogen-bonding interactions that serve to stabilize the Fis1 arm with α2 and α4 on the concave surface, involving Lys89 on α4 and the backbone carbonyls of Ala13, Ile50 and Lys51. These interactions stabilize the inhibitory state of the Fis1 arm. (*c*) The side-chain amide group of Gln112 forms reciprocal hydrogen bonds with the backbone amide of Trp7. This interaction is broken upon complexation (see text). This figure was generated in *PyMOL* (DeLano, 2002).

Dnm1 (Griffin *et al.*, 2005; Lackner *et al.*, 2009; Koirala *et al.*, 2010). In biochemical pulldown experiments, an ∼25% decrease in Mdv1 binding was observed upon removal of the Fis1 arm (Wells *et al.*, 2007). Crystal structures of Fis1ΔTM in complex with peptides derived from Caf4 and Mdv1 have been solved at 1.88 and 2.15 Å resolution, respectively (Zhang & Chan, 2007), and we compared these structures with that of Fis1 alone in order to evaluate whether Fis1 undergoes a conformational change upon peptide binding that might indicate Fis1-mediated allosteric regulation of the fission-machine assembly. However, we observed little gross structural change, with r.m.s.d.s of 0.79 and 1.14 Å for the C^{α} atoms of residues 5–127 between Fis1 and Fis1–Caf4 (red, Fig. 3*d*) and between Fis1 and Fis1–Mdv1 (blue; Fig. 3*e*), respectively. As expected, the largest differences occurred in the Fis1 arm, with a 1.64 Å C^{α}-atom r.m.s.d. between Fis1 and Fis1–Caf4. Two of the four hydrogen bonds found in *LIGPLOT* analysis of the apo Fis1 structure remained the same in both complexes (Pro8–Tyr81 and Ala13–Lys89). The remaining two hydrogen bonds found in the apo Fis1 structure involved Trp7 and Gln112 and were not found in the complex; however, a subtle re-arrangement of the indole side chain allowed a different hydrogen-bonding interaction with Glu78. Overall, ligand binding does not induce a significant conformational change in Fis1, although the complexes are derived from peptides and not full-length proteins, which may explain the biochemical binding results.

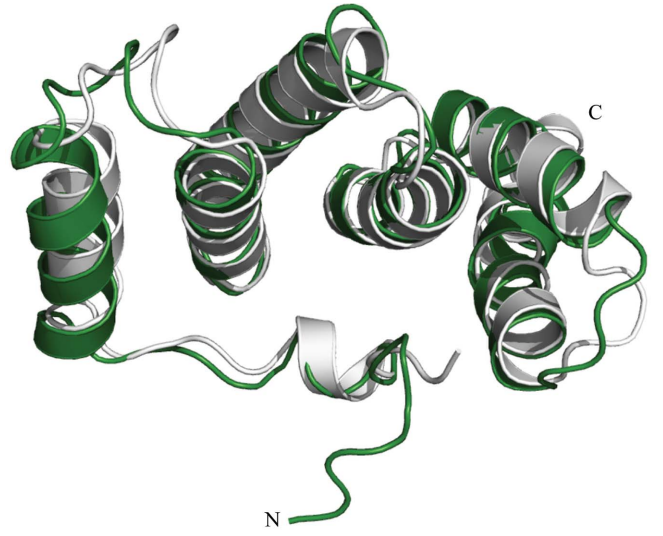

(*a*)

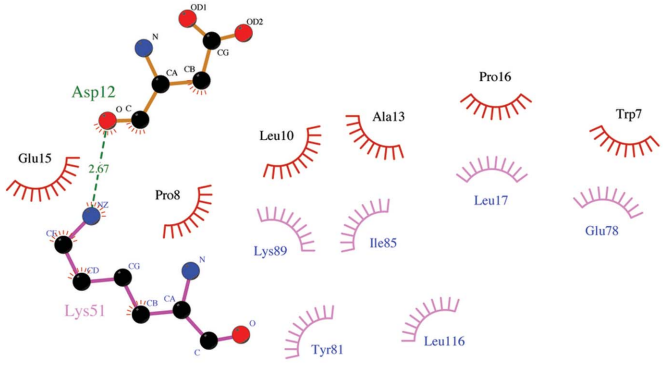

(*b*)

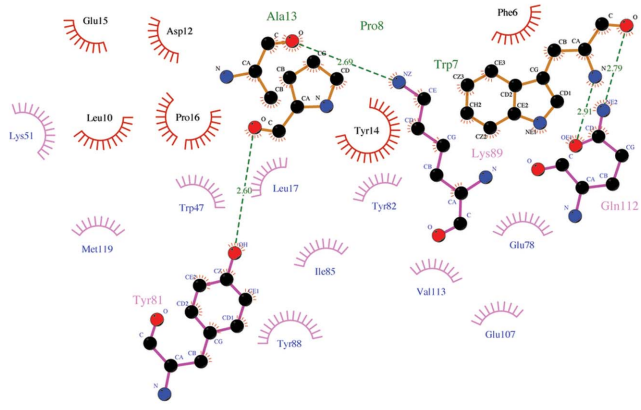

(*c*)

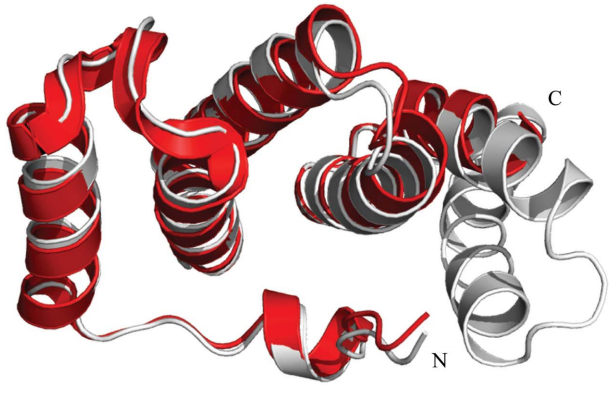

(*d*)

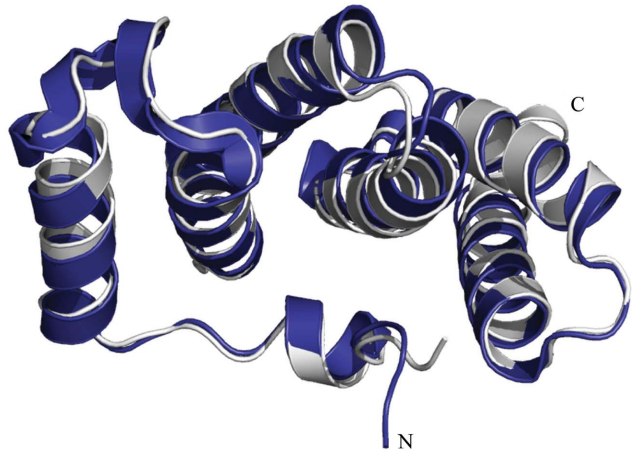

(*e*)

Figure 3
Structural comparisons of the autoinhibitory arm. (*a*) Superposition of the lowest-energy NMR-derived structure (PDB entry 1y8m; green) with that reported here (PDB entry 3o48; white) reveals differences in the orientation of the Fis1 arm that are quantified by *DIMPLOT* (Wallace *et al.*, 1995) analysis of the NMR structure 1y8m (*b*) and the X-ray structure 3o48 (*c*). In (*b*) and (*c*) hydrogen bonds are shown by dashed lines (green) between Fis1-arm (green) and TPR (pink) residues. The length of the bond is indicated in the middle of the dashed line. Hydrophobic interactions are shown by spoked arcs between residues of the Fis1 arm (residues in black with red arcs and spokes) and TPR (residues in blue with pink arcs and spokes). Default criteria were used for determining hydrogen bonds and hydrophobic interactions (Wallace *et al.*, 1995). (*d*) Superposition of Fis1 molecules from a complex with Caf4p (PDB entry 2pqr; red) with that reported here (PDB entry 3o48; white). Note that the ligand is not shown. (*e*) Superposition of Fis1 molecules from a complex with Mdv1p (PDB entry 2pqn; red) with that reported here (PDB entry 3o48, white). Note that the ligand is not shown. This figure was generated using *PyMOL* (DeLano, 2002).

Based on NMR and chemical modification studies, the Fis1 arm exists in a pH-dependent dynamic equilibrium (Picton *et al.*, 2009). At pH 5 the thermodynamic stability of Fis1 is nearly 8 kJ mol^{-1} higher than at pH 7 and structural changes in Fis1 between these two pH values are clustered in the Fis1 arm and proximal regions (Picton *et al.*, 2009). Given the importance of the Fis1 arm in regulating interactions, we have investigated this pH dependence and found that it involves the sole histidine of Fis1, His106, which is located at the C-terminal end of helix 5 and is proximal to the Fis1 arm (Picton *et al.*, 2009). In our pH 7.4 structure the imidazole side chain is not engaged in any specific interactions. However, we find that one of the backbone-dependent rotamers (Dunbrack & Cohen, 1997) of His106 places it in a favorable C-capping interaction with the backbone carbonyl of Thr102. This possibility might provide a structural mechanism for the pH-dependent regulation of the Fis1 arm. In this mechanism, protonation of His106 favors C-capping and stabilization of the Fis1 fold, favoring the autoinhibitory state, whereas deprotonation would break the C-capping interaction and provide relief of autoinhibition. Whether this mechanism is important physiologically is not known, but it supports the idea that Fis1 may be poised to respond to a protein–protein interaction or post-translational modification that triggers relief of autoinhibition.

We gratefully acknowledge Drs Emily Coonrod and Janet M. Shaw for providing Fis1 plasmids for this study. Crystallographic data were obtained on beamline X25 of the Brookhaven National Synchrotron Light Source. Financial support comes principally from the Offices of Biological and Environmental Research and of Basic Energy Sciences of the US Department of Energy and from the National Center for Research Resources of the National Institutes of Health, grant No. P41RR012408. This work was supported by NIH grant R01GM067180 (to RBH).

References

Blatch, G. L. & Lässle, M. (1999). *Bioessays*, **21**, 932–939.
Cerveny, K. L. & Jensen, R. E. (2003). *Mol. Biol. Cell*, **14**, 4126–4139.
Chan, D. C. (2007). *N. Engl. J. Med.* **356**, 1707–1709.
Chen, V. B., Arendall, W. B., Headd, J. J., Keedy, D. A., Immormino, R. M., Kapral, G. J., Murray, L. W., Richardson, J. S. & Richardson, D. C. (2010). *Acta Cryst.* D**66**, 12–21.
Cortajarena, A. L. & Regan, L. (2006). *Protein Sci.* **15**, 1193–1198.
D'Andrea, L. D. & Regan, L. (2003). *Trends Biochem. Sci.* **28**, 655–662.
DeLano, W. L. (2002). *PyMOL*. http://www.pymol.org.
Dohm, J. A., Lee, S. J., Hardwick, J. M., Hill, R. B. & Gittis, A. G. (2004). *Proteins*, **54**, 153–156.
Dunbrack, R. L. & Cohen, F. E. (1997). *Protein Sci.* **6**, 1661–1681.
Emsley, P., Lohkamp, B., Scott, W. G. & Cowtan, K. (2010). *Acta Cryst.* D**66**, 486–501.
Fekkes, P., Shepard, K. A. & Yaffe, M. P. (2000). *J. Cell Biol.* **151**, 333–340.
Griffin, E. E., Graumann, J. & Chan, D. C. (2005). *J. Cell Biol.* **170**, 237–248.
Jofuku, A., Ishihara, N. & Mihara, K. (2005). *Biochem. Biophys. Res. Commun.* **333**, 650–659.
Kabsch, W. (2010). *Acta Cryst.* D**66**, 125–132.
Karren, M. A., Coonrod, E. M., Anderson, T. K. & Shaw, J. M. (2005). *J. Cell Biol.* **171**, 291–301.
Koch, A., Yoon, Y., Bonekamp, N. A., McNiven, M. A. & Schrader, M. (2005). *Mol. Biol. Cell*, **16**, 5077–5086.
Koirala, S., Bui, H. T., Schubert, H. L., Eckert, D. M., Hill, C. P., Kay, M. S. & Shaw, J. M. (2010). *J. Cell Biol.* **191**, 1127–1139.
Lackner, L. L., Horner, J. S. & Nunnari, J. (2009). *Science*, **325**, 874–877.
Long, F., Vagin, A. A., Young, P. & Murshudov, G. N. (2008). *Acta Cryst.* D**64**, 125–132.
Motley, A. M., Ward, G. P. & Hettema, E. H. (2008). *J. Cell Sci.* **121**, 1633–1640.
Mozdy, A. D., McCaffery, J. M. & Shaw, J. M. (2000). *J. Cell Biol.* **151**, 367–380.
Murshudov, G. N., Skubák, P., Lebedev, A. A., Pannu, N. S., Steiner, R. A., Nicholls, R. A., Winn, M. D., Long, F. & Vagin, A. A. (2011). *Acta Cryst.* D**67**, 355–367.
Painter, J. & Merritt, E. A. (2005). *Acta Cryst.* D**61**, 465–471.
Picton, L. K., Casares, S., Monahan, A. C., Majumdar, A. & Hill, R. B. (2009). *Biochemistry*, **48**, 6598–6609.
Robinson, H., Soares, A. S., Becker, M., Sweet, R. & Héroux, A. (2006). *Acta Cryst.* D**62**, 1336–1339.
Schrader, M. (2006). *Biochim. Biophys. Acta*, **1763**, 531–541.
Serasinghe, M. N., Seneviratne, A. M., Smrcka, A. V. & Yoon, Y. (2010). *J. Biol. Chem.* **285**, 620–630.
Serasinghe, M. N. & Yoon, Y. (2008). *Exp. Cell Res.* **314**, 3494–3507
Suzuki, M., Jeong, S.-Y., Karbowski, M., Youle, R. J. & Tjandra, N. (2003). *J. Mol. Biol.* **334**, 445–458.
Suzuki, M., Neutzner, A., Tjandra, N. & Youle, R. J. (2005). *J. Biol. Chem.* **280**, 21444–21452.
Tieu, Q. & Nunnari, J. (2000). *J. Cell Biol.* **151**, 353–366.
Tieu, Q., Okreglak, V., Naylor, K. & Nunnari, J. (2002). *J. Cell Biol.* **158**, 445–452.
Wallace, A. C., Laskowski, R. A. & Thornton, J. M. (1995). *Protein Eng.* **8**, 127–134.
Wells, R. C., Picton, L. K., Williams, S. C., Tan, F. J. & Hill, R. B. (2007). *J. Biol. Chem.* **282**, 33769–33775.
Winn, M. D., Murshudov, G. N. & Papiz, M. Z. (2003). *Methods Enzymol.* **374**, 300–321.
Yoon, Y., Krueger, E. W., Oswald, B. J. & McNiven, M. A. (2003). *Mol. Cell. Biol.* **23**, 5409–5420.
Zhang, Y. & Chan, D. C. (2007). *Proc. Natl Acad. Sci. USA*, **104**, 18526–18530.